

# Lattice model of adsorption in disordered porous materials: Mean-field density functional theory and Monte Carlo simulations

L. Sarkisov and P. A. Monson\*

*Department of Chemical Engineering, University of Massachusetts, Amherst, Massachusetts 01003*

(Received 19 June 2000; revised manuscript received 18 June 2001; published 17 December 2001)

We present mean-field density functional theory calculations and Monte Carlo simulations for a lattice model of a fluid confined in a disordered porous material. The model is obtained by a coarse graining of an off-lattice model of adsorption of simple molecules in silica xerogels. In some of our calculations a model of a porous glass is also considered. The lattice models exhibit behavior that is qualitatively similar to that of their off-lattice counterparts but the computations required are much more tractable and this makes it feasible to investigate the effects of porous material microstructure at longer length scales. We focus on exploring in detail the behavior in the adsorption/desorption hysteresis region for these models. In agreement with recent results for a model that uses a random distribution of solid sites on the lattice [Kierlik *et al.*, Phys. Rev. Lett. **87**, 055701 (2001)] we show that the disorder of the solid matrix induces multiple metastable states within the hysteresis region, which are evident in both the mean-field theory calculations and the Monte Carlo simulations. These multiple metastable states can be connected by scanning curves that are very similar to those seen in experimental studies of adsorption hysteresis. The results from mean-field theory predict that while there is hysteresis in the adsorption/desorption isotherms it is not possible to locate a condition of phase equilibrium that satisfies thermodynamic consistency. A wider significance of these results is discussed.

DOI: 10.1103/PhysRevE.65.011202

PACS number(s): 61.20.Gy, 05.70.Fh, 64.60.Fr

## I. INTRODUCTION

There has been significant progress in developing molecular models of disordered materials [1–8]. Recent simulation studies on these models show that a fluid adsorbed in a disordered porous medium experiences a number of effects, such as confinement, wetting, disorder, etc. that are strongly coupled with each other [5–8]. The main drawback of these models of disordered porous materials is their relative computational complexity. This becomes a crucial issue for problems where we are interested in studying a broad array of morphologies and parameters of a system. Moreover, phase transitions in these systems may involve very large length scales, and it is important to consider a system of a sufficiently large size. Again, in the case of detailed continuous models we quickly reach the limit on how large systems we can consider due to the computational restrictions. This has been a motivation to look for more efficient models and methods, which, at the same time, would preserve the physics associated with the disorder. From this standpoint, lattice models offer two major advantages: (i) they are very efficient from computational point of view; (ii) they allow a relatively simple theoretical treatment.

Lattice models have been applied to various problems in adsorption on surfaces and in porous materials and we can mention here only a sample of the many studies in the literature. Wetting, prewetting and layering transitions on planar solid surfaces have been studied using the mean-field theory [9,10] and Monte Carlo simulation [11]. Recently mean-field lattice-gas models have been used to study the phase behavior of fluids confined between chemically corrugated sub-

strates [12,13]. A lattice model in combination with a mean-field theory has been also applied to study hysteresis in narrow pores [14].

Disordered porous materials have also been studied using lattice models. For instance, a lattice-gas model of a fluid confined in a model of disordered porous material using mean-field predictions and the replica symmetric Ornstein-Zernike (RSOZ) formalism [15]. Other examples are provided by the work of MacFarland *et al.* [16], who considered equilibrium phase transitions of a fluid confined in a model porous medium constructed in a simulation of spinodal decomposition, by Salazar *et al.* [17] who considered a lattice model of adsorption in an aerogel, and by Stauffer and Pandey [18], who considered binary fluid demixing transitions in a gel.

In this paper we focus on developing a lattice model of a disordered porous material that would incorporate a structural and energetical heterogeneity of real materials. The lattice Hamiltonian used in this work is the same as that formulated by Kierlik *et al.* [15] in their work on the RSOZ theories. The difference between our model and theirs lies in a more realistic description of the porous material microstructure. Our model is a coarse graining of an off-lattice model of silica xerogels [4,5,7]. It has a complex three-dimensional interconnected pore space that spans the system over periodic boundaries. This makes this model a good match for studying various effects associated with confinement that are strongly coupled and occur on a large scale. For this model we can formulate a mean-field density functional theory, which permits to study a broad array of system conditions in a computationally effective way.

One of the original goals of this work was to systematically explore the phase behavior of a fluid confined in a disordered morphology. The motivation for this study came from our previous work [27], where we established a link

\*Author to whom correspondence should be addressed.

between confined fluid phase diagrams and the corresponding adsorption behavior for a model of silica xerogel. The lattice model approach to this problem would provide a more extensive and fundamental understanding of this link for a variety of systems and conditions. However, in work done in collaboration with our colleagues at Jussieu [19] it became evident that the picture of the confined fluid behavior might be more complex than originally supposed. In that work [19], mean-field density functional theory was applied to the original model of Kierlik *et al.* [15] in which a random distribution of sites on the lattice is used to model the solid. An important feature was the discovery of a large multiplicity of solutions of the mean-field equations in the hysteresis region of the adsorption/desorption isotherms. The existence of these solutions, which represent local minima of the grand potential, makes it possible to model the scanning behavior seen in the hysteresis region of adsorption/desorption isotherms for materials, such as vycor glasses [20]. Moreover, the theory predicts that hysteresis may occur with or without an equilibrium capillary condensation phase transition. In the present work we show that these important conclusions are sustained when a more realistic description of the porous microstructure is used. The results provide a further indication that the problem of hysteresis in disordered porous materials may be understood entirely within the context of a statistical mechanics in the grand canonical ensemble without invoking transport concepts or an arbitrary description of the connectivity of the void space in the porous material.

## II. MODEL

The lattice model we consider is based on a particulate model of a silica xerogel used in previous works [4,5,7]. The porous material is treated as a matrix of spherical particles in a configuration from a hard sphere system. Our lattice model is a coarse grained version of this system using an fcc lattice for the discretization. The coarse graining is illustrated for a two-dimensional square lattice in Fig. 1. After the coarse graining the system consists of lattice agglomerates of approximately spherical shape. The size of the fcc lattice grid was chosen to keep the ratio of the cluster size to a single lattice site size roughly equal to the analogous ratio for the off-lattice model (a matrix particle size to a fluid particle size). This ratio is about 7. Overall, for a system with 32 matrix agglomerates (the system size considered in our simulation studies of the off-lattice model) we use an fcc lattice with 22 unit cells on each side so that there are 42 592 sites with 13 713 matrix sites. The solid volume fraction is lower for the lattice model than for the off-lattice model, 0.322 vs 0.386. In order to analyze possible system size effects, we also considered a 500-cluster system, obtained in the same fashion as the 32 cluster system. This larger system consisted of 629 856 sites (with 54 unit cells on each side), 214 401 of them matrix site, giving a solid volume fraction of 0.34.

In addition to the above model we have also made some calculations for an fcc lattice model of a porous glass with a solid volume fraction equal to 0.5 and a side length equal to 60 unit cells (864 000 available sites in the system). This system was constructed by spinodal decomposition of the

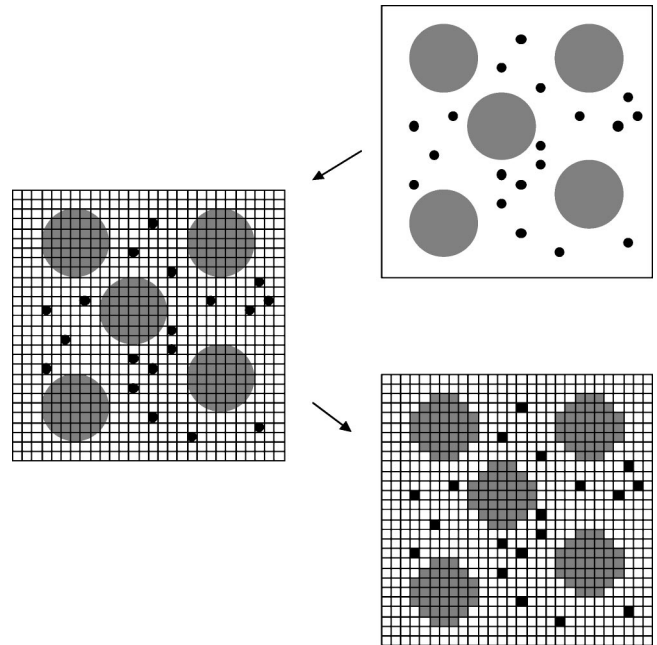


FIG. 1. A schematic representation of the coarse graining used in development of the lattice model.

lattice vapor-liquid system. Spinodal decomposition of a binary alloy system (or a vapor-liquid system for lattice-gas models since these systems are isomorphic for lattices) has been a proven method to generate accurate model structures of porous glasses [21]. This approach has been implemented for both lattice [16] and off-lattice systems [22,6] and schematically works as follows. A system of a fixed composition in a canonical ensemble is equilibrated at a high supercritical temperature (so it has a uniform density). Then it is cooled to a subcritical temperature, where it undergoes spinodal decomposition. It was noticed that the structures the system goes through during this process toward a complete separation indeed resemble those seen for experimental glassy systems. Depending on a desired microstructure, the system is quenched at some point during the decomposition, one of the phases is then removed and the remaining phase serves as an adsorbent matrix. In this work we allowed an equimolar binary alloy system with  $T/T_{c,b} = 0.204$  to spinodally decompose until a desired surface area was obtained. We define the surface area as a fraction of liquid sites in contact with the gas phase and it was set to 0.385 for the system of interest. The decomposition process was modeled via canonical Monte Carlo approach and the low temperature of the system ensured that the separated phases were essentially pure. Then the system was quenched and one phase was removed. The obtained quenched configuration served as a model of porous glass for our adsorption calculations. In Fig. 2 we show computer graphics visualizations for the two morphologies considered in this paper together and for the case of a random distribution of sites on the lattice.

The Hamiltonian we have used is that one formulated by Kierlik *et al.* [15]. In their work they considered a random distribution of matrix sites, but the form of the Hamiltonian remains the same for all matrix morphologies. We have

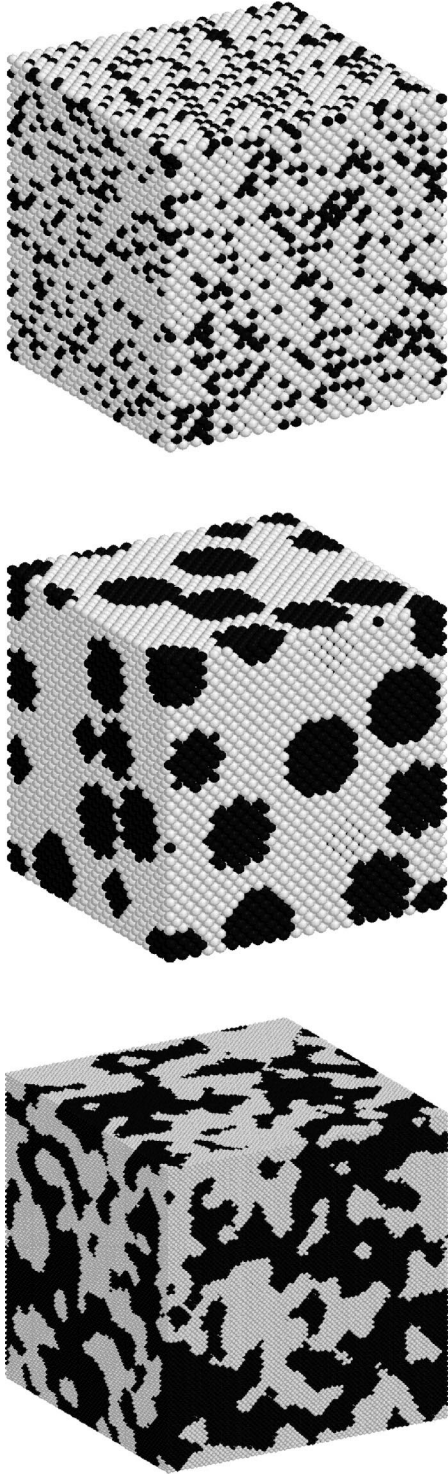


FIG. 2. Computer graphics visualizations of lattice models, from top to bottom: a random model, a model of a silica xerogel, and a model of porous glass. Solid sites are shown in black.

$$H = -\omega_{11} \sum'_{i<j} \tau_i \tau_j \eta_i \eta_j - \omega_{01} \sum'_{i<j} [\tau_i \eta_i (1 - \eta_j) + \tau_j \eta_j (1 - \eta_i)], \quad (2.1)$$

where  $\tau_i = 1$  if site  $i$  is occupied by a fluid particle and  $\tau_i$

$= 0$  if it is not. Similarly  $\eta_i = 0$  if site  $i$  is occupied by a matrix particle and  $\eta_i = 1$  if it is not. The primed summations denote the restriction to pairs of sites that are nearest neighbors. For all considered morphologies we used solid-fluid interaction parameter  $\alpha = \omega_{01} / \omega_{11} = 1.25$ .

### III. MEAN-FIELD DENSITY FUNCTIONAL THEORY

The density functional treatment presented here is similar to the one used in previous work going back to that of de Oliveira and Griffiths [9] and Ebner [10] for adsorption on planar solid surfaces. We express the current state of a site as an average occupancy at this site plus a fluctuation about the average. We have

$$\tau_i \eta_i = \rho_i + \delta \rho_i = \rho_i + (\tau_i \eta_i - \rho_i). \quad (3.1)$$

After neglecting terms beyond linear in the fluctuation we can write

$$\tau_i \tau_j \eta_i \eta_j = -\rho_i \rho_j + \rho_i \tau_i \eta_j + \rho_j \tau_j \eta_i. \quad (3.2)$$

This allows us to rewrite Eq. (2.1) as

$$H_{mf} = -H_0 - \sum_i \tau_i \eta_i \left\{ \sum'_j [\omega_{11} \rho_j + \omega_{01} (1 - \eta_j)] \right\}, \quad (3.3)$$

where the primed sum over  $j$  denotes a sum over the sites that are nearest neighbors of the site  $i$  and

$$H_0 = -\omega_{11} \sum'_{i<j} \rho_i \rho_j. \quad (3.4)$$

We can write the grand partition function of the system as

$$\Xi = \sum_{\{\tau\}} \exp[-\beta(H_{mf} - \mu N)] = e^{\beta H_0} \sum_{\{\tau\}} \prod_i e^{\tau_i X_i}, \quad (3.5)$$

where  $\{\tau\}$  denotes the set of values of  $\tau$  for all lattice sites. Here it is important to notice that the last product in Eq. (3.5), which goes over all sites, becomes equivalent to the one that goes only over sites that are not occupied by matrix, since for sites occupied by matrix  $\tau_i = 0$  and the corresponding term in the product is unity. From now on we will restrict the sums and products to sites unoccupied by the solid. Then we have

$$e^{\beta H_0} \sum_{\{\tau\}} \prod_i e^{\tau_i X_i} = e^{\beta H_0} \prod_i \sum_{\{\tau\}} e^{\tau_i X_i} = e^{\beta H_0} \prod_i [1 + e^{X_i}]. \quad (3.6)$$

The quantity  $X_i$  is given by

$$X_i = \beta \left\{ \sum'_j [\omega_{11} \rho_j + \omega_{01} (1 - \eta_j)] + \mu \right\}. \quad (3.7)$$

The grand potential is given by

$$\Omega = -\frac{1}{\beta} \left[ \beta H_0 + \sum_i \ln(1 + e^{X_i}) \right], \quad (3.8)$$

where the sum over  $i$  is restricted to sites unoccupied by the matrix. The local density at site  $i$  may be determined from the partial derivative of the grand potential with respect to the intrinsic chemical potential [23]

$$\rho_i = - \left( \frac{\partial \Omega}{\partial (\mu - v_i)} \right)_{T,V} = \frac{1}{[1 + e^{-X_i}]}, \quad (3.9)$$

where  $\Omega$  is the grand potential of the system and

$$v_i = -\omega_{01} \sum_j' (1 - \eta_j) \quad (3.10)$$

is the external field on site  $i$ . Equation (3.9) also satisfies the necessary condition for the minimum value of the grand potential, i.e.,

$$\left( \frac{\partial \beta \Omega}{\partial \rho_i} \right)_{T,V} = 0 \quad (3.11)$$

for all  $i$ . Our expressions may be shown to be equivalent to those used in earlier work on the mean-field approximation for inhomogeneous lattice fluids [9,10,12,13]. The form of Eq. (3.9) shows that for a lattice of  $M$  sites we have a system of  $M$  nonlinear equations. In this work we use a simple iteration procedure starting from an initial density for each site.

Here, so far, we have derived expressions for a grand canonical ensemble. It is also possible to perform these calculations in the canonical ensemble. A similar approach has been recently employed by several groups [24,25]. Now, instead of  $T$  and  $\mu$ , we keep constant  $T$  and  $\rho$ . The problem is then to minimize the free-energy functional  $F([\rho_i])$  under a restriction of constant density, i.e.,  $\sum_i \rho_i = M\rho$ . One can show that it leads to a double iteration: we first solve a system of equations for the fluid density identical to those for the grand canonical ensemble (3.9), and then adjust chemical potential

$$\mu^{n+1} = \mu^n + kT \ln \left( \frac{M\rho}{\sum_i \rho_i} \right) \quad (3.12)$$

to accommodate constant density condition. Here  $n$  corresponds to the outer iteration loop. Then we repeat the fluid density iteration procedure. As has been shown for planar substrates, this approach can be used to reveal additional metastable states, forming multiple van der Waals-like loops [24].

#### IV. MONTE CARLO SIMULATIONS

We have carried out Monte Carlo simulations of the model described in Sec. II using the Metropolis method [26] in the grand canonical ensemble. Our Monte Carlo simulations were generally carried out over 5000 moves per lattice site for sites unoccupied by solid, one half of which were

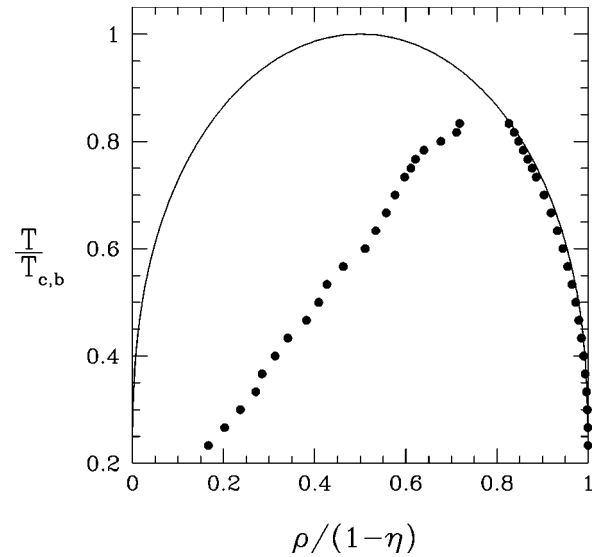


FIG. 3. Temperature ( $T/T_{c,b}$ ) vs density ( $\rho/(1-\eta)$ ) phase diagrams for the lattice model of a fluid confined in a xerogel material with  $\omega_{01}/\omega_{11}=1.25$  calculated via the mean-field theory (filled circles) and compared with that of a bulk fluid (line).

used for equilibration of the system and the other half for averaging. Some tests with much longer runs indicated that runs of this length were sufficient to obtain reproducible results for the states considered in this work. However, longer runs would be needed to make quantitative studies in the near critical region. In calculating adsorption isotherms we started from a state of low activity and carried out a sequence of simulations for progressively increasing activity using the final configuration at each state as the initial configuration for the next state. Desorption isotherms were calculated by starting at a high activity state and carrying out a sequence of simulations for progressively decreasing activity, again using the final configuration at each state as the initial configuration for the next state.

#### V. RESULTS

We begin this chapter by presenting confined fluid phase behavior calculations for the xerogel model. For all the calculations we consider a case with solid-fluid interaction parameter  $\alpha=1.25$ . This is somewhat close to the  $\epsilon_{sf}/\epsilon_{ff}=1.1435$  parameter used for the off-lattice case [5]. Since, there are no long range interactions in the lattice model, this parameter was taken to be slightly higher to imitate a stronger field arising from the range of the solid-fluid interaction in the off-lattice model. In Fig. 3 we show a phase diagram calculated via the mean-field theory approach (filled circles) and bulk coexistence curve (line). This phase diagram calculation is based on the assumption that in the hysteresis region either a fluid state on the adsorption or a fluid state on the desorption branch of an isotherm corresponds to a state of global grand potential minimum. In this case the phase diagram calculation procedure is straightforward and is based on search for the following condition in the hysteresis region:

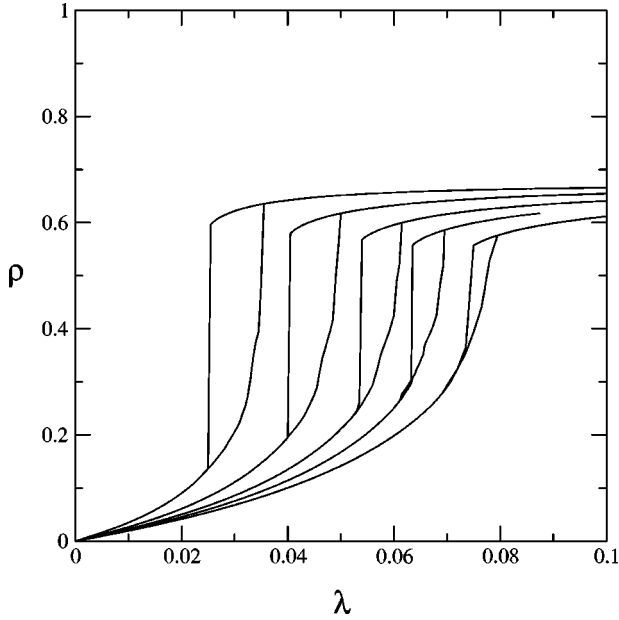


FIG. 4. Adsorption/desorption isotherms of density  $\rho$  vs activity  $\lambda$  at different temperatures  $kT/\omega_{11} = 1.9, 2.1, 2.25, 2.35, 2.45$  (isotherms from left to right, respectively) for the lattice model of a fluid confined in a xerogel material (32 solid clusters) with  $\omega_{01}/\omega_{11} = 1.25$  calculated via the mean-field theory.

$$\mu_1 = \mu_2, \quad (5.1)$$

$$\Omega_1 = \Omega_2, \quad (5.2)$$

where the subscripts denote the two phases in equilibrium. An advantage of the mean-field approach is that it allows us to calculate the grand potential directly and this is why we thought this approach would be such a great tool for quick qualitative phase behavior calculations. A more detailed analysis shows, however, that the states on the adsorption and desorption branches of a hysteresis loop are not the only states possible in the system, and, moreover, they do not necessarily correspond to the global grand potential minimum for a given chemical potential [19]. Thermodynamic consistency requires, that we should be also able to calculate the grand potential density by integrating the Gibbs adsorption equation

$$d\Omega = -M\rho_f d\mu \quad (5.3)$$

starting from a point where grand potential is known. As long as the integration path involves only equilibrium states and does not pass through phase transitions, the calculated grand potential is expected to be identical to that calculated directly. This idea can be tested directly in the mean-field theory [19]. This test applied to the systems considered here shows that the discrepancy between the thermodynamic properties begins as soon as we enter the hysteresis region.

Another way to show this is to focus on the identification of additional metastable states in the system and to search for a true locus of grand potential minima. Before exploring this subject in more detail it is useful to present several examples of adsorption isotherms of the xerogel model. In Fig. 4 we

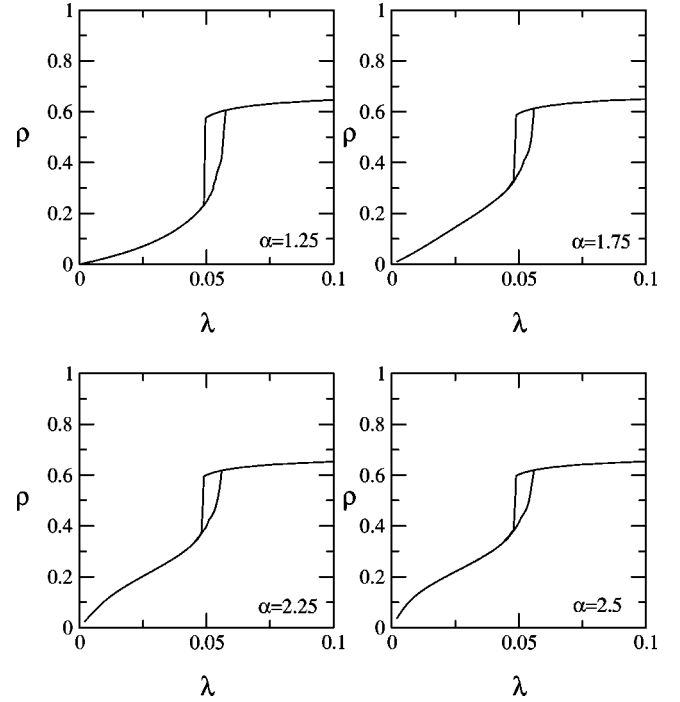


FIG. 5. Adsorption/desorption isotherms of density  $\rho$  vs activity  $\lambda$  at  $kT/\omega_{11} = 2.2$  for the lattice model of a fluid confined in a xerogel material (32 solid clusters) with different strengths of solid-fluid interaction  $\alpha = \omega_{01}/\omega_{11} = 1.25, 1.75, 2.25, 2.5$  (clockwise starting from upper left isotherm) calculated via the mean-field theory.

show adsorption isotherms calculated for various temperatures at  $\alpha = 1.25$ . In Fig. 5 we show the influence of increasing  $\alpha$  on the shape of an isotherm at  $T^* = 2.2$ . The isotherms are very similar to those seen experimentally for adsorption in silica xerogels [28].

We have conducted a search for additional local minima of the grand potential in the hysteresis region using two approaches. First we have done constant average density calculations at various values of the average density in the hysteresis region. We have also calculated scanning curves for sequences of increasing or decreasing the chemical potentials starting from several states on the hysteresis loop. In Fig. 6 we present results for our model xerogel system. The upper left graph shows an adsorption isotherm for the xerogel system at  $T^* = 2.5$  (lines). The upper right graph shows the expanded hysteresis region from the upper left graph (lines and closed circles). In the lower right graph we also show data from constant density calculations. The lower left graph shows again the adsorption isotherm expanded in hysteresis region for  $T^* = 2.5$  ( $T/T_{c,b} = 0.8333$ ) along with scanning curves. In both cases we see that there are many solutions of the mean-field equations in the hysteresis region. The multiple solutions of the mean-field equations for these systems correspond to multiple local minima of the grand potential. The occurrence of these local minima is associated with the complexity of the potential energy landscape in these disordered systems [19].

This picture is further confirmed by calculations for a system with an fcc arrangement of matrix particles where we observed only a small limited number of additional meta-

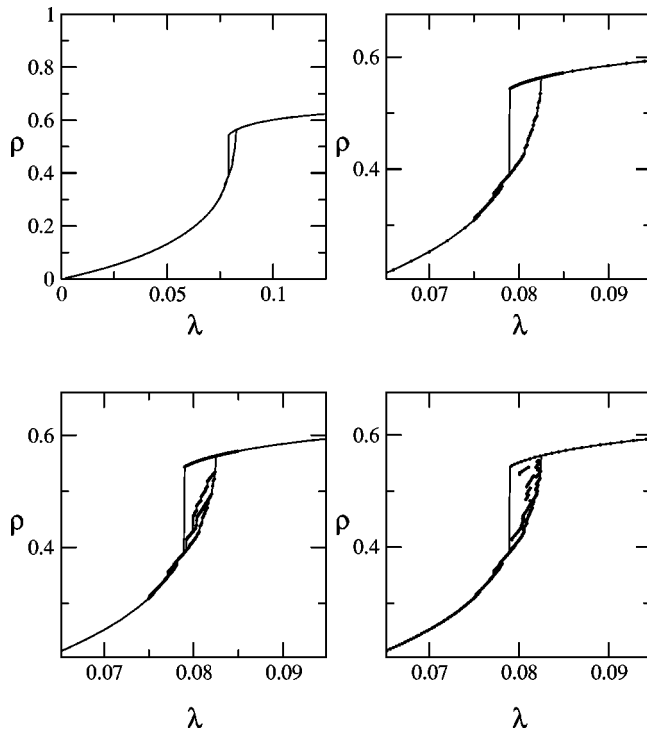


FIG. 6. Adsorption/desorption isotherm of density  $\rho$  vs activity  $\lambda$  at  $kT/\omega_{11}=2.5$  for the lattice model of a fluid confined in a xerogel material (32 solid clusters) with  $\omega_{01}/\omega_{11}=1.25$  calculated via the mean-field theory. Upper left graph shows the isotherm (lines). Upper right graph shows the expanded hysteresis region (lines and filled circles). Lower graphs show additional metastable states from constant density calculations (right) and from scanning curves (left).

stable states, that included states associated with layering and interparticle bridging. Due to a relatively weak solid-fluid interaction, these states were observed only at very low temperatures and belonged to a metastable part of the adsorption branch. The transitions we observed for the ordered matrix are akin to wetting and prewetting transitions studied by Dobbs and Yeomans for two neighboring spheres [29].

Unlike for some of the random matrix systems [19], in Fig. 6 the metastable states appear not to fill the entire hysteresis region. However, further calculations revealed that this was partly related to the system size. In Fig. 7, the upper graph shows an adsorption isotherm expanded in the hysteresis region for a larger system size at the same temperature and also additional states obtained from scanning curves. There are two important features of this graph. The desorption branch of the hysteresis loop appears to be continuous and the scanning curves span most of the hysteresis region. The lower graph of Fig. 7 shows another example of this behavior at  $T^*=2.55$  ( $T/T_{c,b}=0.85$ ). With a larger system we have a larger sample of the disorder and we should thus expect a larger number of solutions to the mean-field equations.

So far, our discussion of the hysteresis region has involved only mean-field calculations. In order to confirm that these additional metastable states are not an artifact of the

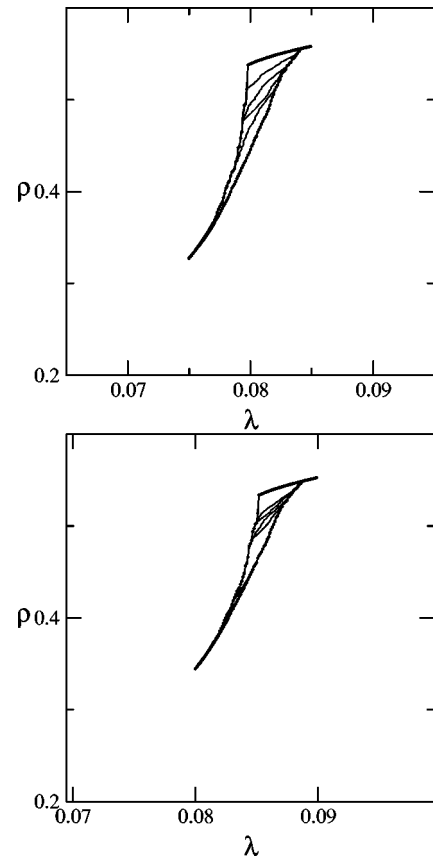


FIG. 7. Expanded hysteresis region of an adsorption/desorption isotherm and scanning curves of density  $\rho$  vs activity  $\lambda$  at  $kT/\omega_{11}=2.5$  (the upper graph) and  $kT/\omega_{11}=2.55$  (the lower graph) for the lattice model of a fluid confined in a xerogel material (500 solid clusters) with  $\omega_{01}/\omega_{11}=1.25$  calculated via the mean-field theory.

mean field theory we have performed additional calculations using grand canonical Monte Carlo simulations. In each case the system was equilibrated at each point the system was run for up to 5000 moves per lattice site at each activity. Results are shown in Fig. 8. The upper graph corresponds to the 32-cluster xerogel system at  $T^*=1.8$  ( $T/T_{c,b}=0.735$ ). The lower graph corresponds to the 500-cluster xerogel system at  $T^*=1.8$ . Both graphs show additional metastable states calculated in scanning sequences. It is less clear for the smaller system, but again this seems to be a system size effect only. For a 500-cluster system we see clear scanning behavior.

Finally, we present mean-field theory (MFT) calculations for a lattice model of a porous glass [16]. In Fig. 9, the graph shows an isotherm for a glass system with solid volume fraction equal to 0.5,  $\alpha=1.25$  at  $T^*=2.35$  ( $T/T_{c,b}=0.783$ ) and several scanning curves initiated on adsorption. Again, there is a clear evidence of additional metastable states. This observation suggests the generality of the picture emerging from these calculations and the earlier ones [19]. The multiplicity of metastable states is determined by porous media disorder and is an intrinsic feature of all disordered morphologies. The trend we have observed for the confined fluid behavior with the increasing system size leads us to speculate that a system of a macroscopic size would induce an

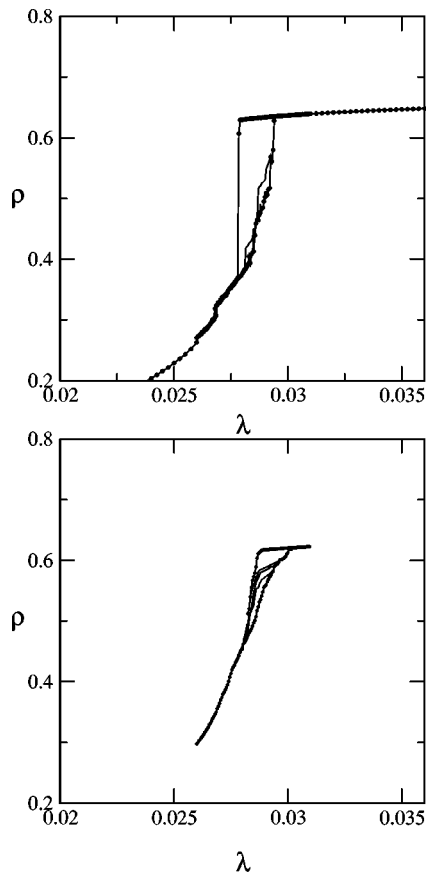


FIG. 8. Expanded hysteresis region of an adsorption/desorption isotherm and scanning curves of density  $\rho$  vs activity  $\lambda$  at  $kT/\omega_{11} = 1.8$  for the lattice model of a fluid confined in a xerogel material (32 solid clusters - upper graph; 500 solid clusters - lower graph) with  $\omega_{01}/\omega_{11} = 1.25$  calculated via grand canonical Monte Carlo simulations.

infinite number of metastable states within the hysteresis region. We have found that this effect also occurs after averaging over several realizations of the solid matrix disorder [30]. Once these multiple states are identified it is possible to search for a grand potential minimum. Our preliminary analysis shows that the systems described here exhibit no sharp transition similar to the vapor-liquid transition in bulk fluid. At the same time the necessity to uniquely identify phases in coexistence is no longer obvious. Given the large number of states with closely spaced grand potentials, a system may never actually reach the states of phase coexistence, although they correspond to the thermodynamic equilibrium.

## VI. CONCLUSIONS

We have presented some results for lattice models of disordered porous materials focusing primarily on a model developed by a coarse graining of an off-lattice model of a silica xerogel. The model has several key features, specifically it incorporates a three-dimensional complexity of real porous structures, it is computationally efficient and it allows

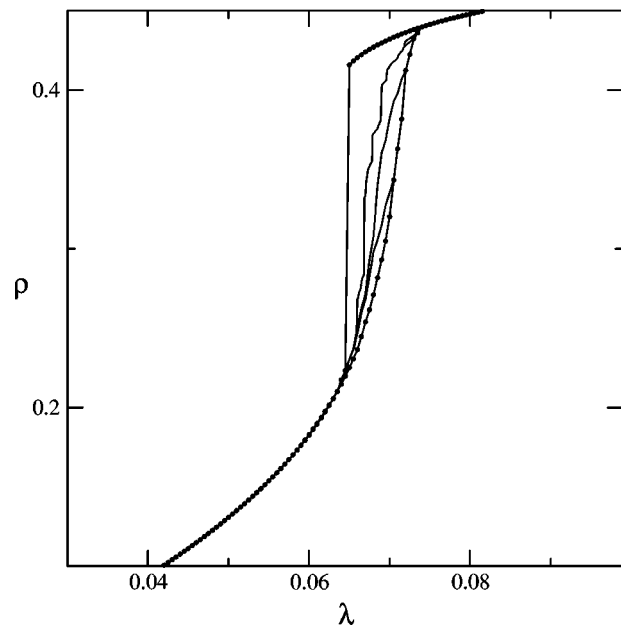


FIG. 9. Expanded hysteresis region of an adsorption/desorption isotherm and scanning curves of density  $\rho$  vs activity  $\lambda$  at  $kT/\omega_{11} = 2.35$  for the lattice model of a fluid confined in a porous glass with  $\omega_{01}/\omega_{11} = 1.25$  calculated via the mean-field theory (lines and closed circles).

a simple theoretical treatment. The thermodynamic properties have been studied by the mean-field density functional theory and Monte Carlo simulation. The behavior of the models in the hysteresis region is very interesting and is in qualitative agreement with experimental results for adsorption isotherms of simple gases in xerogels and porous glasses [20] including the observation of scanning curves. Moreover, it confirms the picture emerging from a recent study of a model with a random distribution of the solid sites on the lattice [19].

The present results indicate that for the lattice models of xerogels and porous glasses considered here in both the MFT and Monte Carlo simulations the hysteresis behavior is not associated with a simple van der Waals-like metastability accompanying a first order vapor-liquid transition [19]. Whether or not this suggestion applies to the off-lattice versions of these models [5,6,31–33] remains to be seen. However, given the similarities of the calculated phase diagrams for the lattice and off-lattice models of the silica xerogel it is quite plausible that it does. The question of whether there is a true phase transition in these systems is thus more subtle than envisaged by recent theoretical [31] and simulation studies [5,32,33].

Finally, we want to make reference to a recent simulation study [34] of an off-lattice model where we showed that the hysteresis obtained in grand canonical Monte Carlo simulations could be reproduced by a molecular dynamics algorithm in which adsorption and desorption occur via diffusive mass transfer. These calculations together with this and our other recent work [19] indicate that we can learn a great deal

about adsorption hysteresis using statistical mechanics in the grand canonical ensemble, provided that the porous material microstructure is modeled in a realistic manner. This is achieved without making assumptions about the connectivity of the void space or by introducing percolation concepts [35–37].

## ACKNOWLEDGMENTS

This work was supported by the National Science Foundation (Grant Nos. CTS-9700999 and CTS-9906794). We are grateful to M. L. Rosinberg, E. Kierlik, and G. Tarjus for useful discussions.

- 
- [1] L. D. Gelb, K. E. Gubbins, R. Radhakrishnan, and M. Sliwiska-Bartowiak, *Rep. Prog. Phys.* **62**, 1573 (1999).
- [2] M. L. Rosinberg, in *New Approaches to Problems in Liquid State Theory*, edited by C. Caccamo *et al.* (Kluwer, Dordrecht, 1999).
- [3] J. M. D. MacElroy and K. Raghavan, *J. Chem. Phys.* **93**, 2068 (1990).
- [4] R. D. Kaminsky and P. A. Monson, *J. Chem. Phys.* **95**, 2936 (1991).
- [5] K. S. Page and P. A. Monson, *Phys. Rev. E* **54**, R29 (1996); **54**, 6557 (1996).
- [6] L. D. Gelb and K. E. Gubbins, *Langmuir* **14**, 2097 (1998).
- [7] L. Sarkisov, K. S. Page, and P. A. Monson, in *Fundamentals of Adsorption*, edited by F. Meunier (Elsevier, Paris, 1998), Vol. 6, pp. 847–853.
- [8] R. J.-M. Pellenq, A. Delville, H. van Damme, and P. Levitz, *Stud. Surf. Sci. Catal.* **128**, 1 (2000).
- [9] M. J. de Oliveira and R. B. Griffiths, *Surf. Sci.* **71**, 689 (1978).
- [10] C. Ebner, *Phys. Rev. A* **22**, 2776 (1980).
- [11] D. B. Nicolaidis and R. Evans, *Phys. Rev. Lett.* **63**, 778 (1989).
- [12] P. Röcken and P. Tarazona, *J. Chem. Phys.* **105**, 2034 (1996).
- [13] H. Bock and M. Schoen, *Phys. Rev. E* **59**, 4122 (1999).
- [14] U. Marini Bettolo Marconi and F. van Swol, *Europhys. Lett.* **8**, 531 (1989).
- [15] E. Pitard, M. L. Rosinberg, G. Stell, and G. Tarjus, *Phys. Rev. Lett.* **74**, 4361 (1995); E. Kierlik, M. L. Rosinberg, G. Tarjus, and E. Pitard, *Mol. Phys.* **95**, 341 (1998).
- [16] T. MacFarland, G. T. Barkema, and J. F. Marko, *Phys. Rev. B* **53**, 148 (1996).
- [17] R. Salazar, R. Toral, and A. Chakrabarti, *J. Sol-Gel Sci. Technol.* **15**, 175 (1999).
- [18] D. Stauffer and R. B. Pandey, *J. Phys. A* **25**, L1079 (1992).
- [19] E. Kierlik, P. A. Monson, M. L. Rosinberg, L. Sarkisov, and G. Tarjus, *Phys. Rev. Lett.* **27**, 055701 (2001).
- [20] C. G. V. Burgess, D. H. Everett, and S. Nuttall, *Pure Appl. Chem.* **61**, 1845 (1989).
- [21] P. Levitz, G. Ehret, S. K. Sinha, and J. M. Drake, *J. Chem. Phys.* **95**, 6151 (1991).
- [22] B. Strickland, G. Leptoukh, and C. Roland, *J. Phys. A* **28**, L403 (1995).
- [23] R. Evans, in *Liquids at Interfaces*, Proceedings of the Les Houches Summer School Session XLVIII, edited by J. Charvolin, J. F. Joanny, and J. Zinn-Justin (Elsevier, Amsterdam, 1990).
- [24] G. L. Aranovich and M. D. Donahue, *Phys. Rev. E* **60**, 5552 (1999).
- [25] A. V. Neimark and P. I. Ravikovitch, *Stud. Surf. Sci. Catal.* **128**, 51 (2000).
- [26] N. Metropolis, A. W. Rosenbluth, M. N. Rosenbluth, A. N. Teller, and E. Teller, *J. Chem. Phys.* **21**, 1087 (1953).
- [27] L. Sarkisov and P. A. Monson, *Phys. Rev. E* **61**, 7231 (2000).
- [28] W. D. Machin, *J. Chem. Soc., Faraday Trans.* **88**, 729 (1992).
- [29] H. T. Dobbs and J. M. Yeomans, *J. Phys.: Condens. Matter* **4**, 10 133 (1992).
- [30] H.-J. Woo, L. Sarkisov, and P. Monson (unpublished).
- [31] E. Kierlik, M. L. Rosinberg, G. Tarjus, and P. A. Monson, *J. Chem. Phys.* **106**, 264 (1997).
- [32] M. Alvarez, D. Levesque, and J.-J. Weis, *Phys. Rev. E* **60**, 5495 (1999).
- [33] P. A. Gordon and E. D. Glandt, *Langmuir* **13**, 4659 (1997).
- [34] L. Sarkisov and P. Monson, *Langmuir* **16**, 9857 (2000).
- [35] G. Mason, *Proc. R. Soc. London, Ser. A* **415**, 453 (1988).
- [36] P. C. Ball and R. Evans, *Langmuir* **5**, 714 (1989).
- [37] N. A. Seaton, *Chem. Eng. Sci.* **46**, 1895 (1991).